Atmos. Chem. Phys. Discuss., 12, 14697–14726, 2012
www.atmos-chem-phys-discuss.net/12/14697/2012/
doi:10.5194/acpd-12-14697-2012

Atmospheric Chemistry and Physics Discussions

Effect of photochemical aging on the ice nucleation properties of diesel and wood burning particles

C. Chou[1,*], O. Stetzer[1], T. Tritscher[2,], R. Chirico[2,***], M. F. Heringa[2], Z. A. Kanji[1], E. Weingartner[2], A. S. H. Prévôt[2], U. Baltensperger[2], and U. Lohmann[1]**

[1]ETH Zurich, Institute for Atmospheric and Climate Science, Switzerland
[2]Laboratory of Atmospheric Chemistry, Paul Scherrer Institute, Villigen PSI, Switzerland
[*]now at: Science and Technology Research Institute, University of Hertfordshire, Hatfield, UK
[**]now at: TSI GmbH, Particle Instruments, Aachen, Germany
[***]now at: Italian National Agency for New Technologies, Energy and Sustainable Economic Development (ENEA), UTAPRAD-DIM, Frascati, Italy

Received: 30 April 2012 – Accepted: 23 May 2012 – Published: 8 June 2012

Correspondence to: C. Chou (c.chou@herts.ac.uk)

Published by Copernicus Publications on behalf of the European Geosciences Union.

Abstract

A measurement campaign (IMBALANCE) was conducted in 2009 and aimed at characterizing the physical and chemical properties of freshly emitted and photochemically aged combustion particles emitted from a log wood burner and diesel vehicles: a EURO3 Opel Astra with a diesel oxidation catalyst (DOC) but no particle filter and a EURO2 Volkswagen Transporter TDI Syncro with no emission after-treatment. Ice nucleation experiments in the deposition and condensation freezing modes were conducted with the Portable Ice Nucleation Chamber (PINC) at three nominal temperatures, −30 °C, −35 °C and −40 °C. Freshly emitted diesel particles showed ice formation only at −40 °C in the deposition mode at 137 % relative humidity with respect to ice (RH_i) and 92 % relative humidity with respect to water (RH_w), and photochemical aging did not play a role in modifying their ice nucleation behavior. Only one diesel experiment where α-pinene was added, showed an ice nucleation enhancement after the aging at −35 °C. Wood burning particles also act as ice nuclei (IN) at −40 °C in the deposition mode at the same conditions as for diesel particles and photochemical aging did also not alter the ice formation properties of the wood burning particles. Unlike diesel particles, wood burning particles form ice via condensation freezing at −35 °C with no ice nucleation observed at −30 °C for wood burning particles. Photochemical aging did not affect the ice nucleation ability of the diesel and wood burning particles at the three different temperatures investigated but a broader range of temperatures below −30 °C need to be investigated in order to draw an overall conclusion on the effect of photochemical aging on deposition/condensation ice nucleation across the entire temperature range relevant to cold clouds.

1 Introduction

Soot particles are solid, carbonaceous products resulting from incomplete combustion of materials such as coal, wood and other fossil fuels. Both wood burning particles from

ACPD
12, 14697–14726, 2012

house heating or cooking and diesel car emissions contribute to a large fraction of particulate matter (PM) in the atmosphere. These combustion particles also consist of several types of volatile organic compounds (VOC) (McDonald et al., 2000; Schauer et al., 2001, 2002). Because combustion particles contain black carbon (BC), they warm the atmosphere by absorbing solar radiation thus reducing the amount of radiation reaching the surface. The reduction in surface heating increases the static stability of the atmosphere and therefore tends to reduce convection and cloud formation (Denman et al., 2007). This change in cloudiness due to the decrease in near-cloud relative humidity and the increase in static stability caused by absorbing aerosol is called the semi-direct aerosol effect (Hansen et al., 1997) and has been observed in the Amazon region by Koren et al. (2004). However, Lin et al. (2006) showed for the same region that a high load of biomass burning could invigorate cloud formation. Recent field studies conducted at the high Alpine research station Jungfraujoch (Cozic et al., 2008; Targino et al., 2009) indicated that carbonaceous material is enriched in ice residuals with respect to the bulk aerosol. This is supported by the results from Ebert et al. (2011) who showed an enrichment in BC in the ice crystals sampled using a scanning electron microscope at the same research site. Nevertheless, the correlation between ice crystal concentration and BC enrichment is still unclear and more investigation is needed, as in a later campaign Kamphus et al. (2010) found that no BC enrichment was observable using a single particle mass spectrometer. In mid-level clouds, precipitation is generally initiated by the ice phase due to the Bergeron-Findeisen process. Lohmann and Hoose (2009) showed for example that a high concentration of BC particles could potentially lead to a faster glaciation of mixed phase clouds inducing earlier precipitation and resulting in a shorter cloud lifetime. Ice formation in clouds can take place via different heterogeneous processes which all involve the presence of a foreign particle termed ice nuclei (IN). Deposition, condensation, immersion and contact nucleation represent the four possible modes of ice nucleation in the atmosphere (Vali, 1985). Deposition nucleation occurs when ice deposits directly from the vapour phase onto the IN. Condensation freezing refers to the condensation of supercooled liquid water on

ACPD
12, 14697–14726, 2012

the IN followed by subsequent freezing of the droplet. Immersion freezing involves first the formation of a droplet around the IN, and upon cooling, the droplet freezes whereas contact freezing refers to the ice formation after the collision of a supercooled droplet with an interstitial solid aerosol.

The contribution of soot particles to deposition nucleation at temperatures above −35 °C is still unclear, as the onset of ice formation is very close to water saturation (DeMott et al., 1999; Möhler et al., 2005b,a; Dymarska et al., 2006). Furthermore, in the atmosphere, aerosol particles undergo a process called aging which refers to different processes such as condensation of soluble materials and oxidized gases on the surface of the particles as well as surface reactions altering the particle chemical composition. These processes can affect the physical properties such as hygroscopicity, light scattering and absorption of the particles as well as their cloud formation ability. The review from Kärcher et al. (2007) summarized the main ice nucleation experiments performed on soot particles at cirrus level temperatures where three different types of soot were investigated (Degussa Soot, flame soot and graphite spark generated soot). In a temperature range from −40 °C to −85 °C, the three different soot particles all showed different ice nucleation properties and graphite spark generated soot was found to be the most efficient ice nucleus in the deposition freezing mode as it required lower relative humidity with respect to ice (RH_i) to reach a 1 % activated fraction. The RH_i required for ice activation of untreated graphite spark soot range from 110 % to 140 % whereas other soot types required more than 140 %. It has also been shown that a sulfuric acid coating on soot particles reduced the ice nucleation efficiency in the temperature range of −40 °C to −85 °C in the deposition mode (Möhler et al., 2005a). Möhler et al. (2005b) showed that a higher organic carbon (OC) content in a soot particle decreases the IN ability at −65 °C by an ice saturation ratio of 0.25 (from 1.45 to 1.7). These studies infer that modification of the surface properties of soot particles can have a direct effect on their ice nucleation ability. Hoose et al. (2008) and Storelvmo et al. (2008) showed that if the coating has the ability to de-activate some IN as it was shown in the study of Möhler et al. (2005b) with sulphuric acid, this would

ACPD
12, 14697–14726, 2012

lead to a lower frequency of cloud glaciation, a delay in precipitation formation and thus a longer cloud life time. The result is an increase in cloud albedo leading to a cooling of the surface.

The IMpact of Biomass burning AerosoL on Air quality aNd ClimatE (IMBALANCE) project aimed at characterizing the physical and chemical properties of aged and non aged biomass burning particles from wood and combustion particles from diesel cars. The measurement campaign took place at the Paul Scherrer Institute's smog chamber from 17 August to 15 October 2009, in Villigen, Switzerland. Ice nucleation experiments took place from 17 August to 23 September 2009. So far, no ice nucleation measurements on the effect of photochemical aging onto wood burning and diesel soot have been reported in the literature as previous coating studies have been performed with laboratory soot generators and were not representative of soot particles found in the atmosphere. This paper discusses the ice nucleation properties of fresh and photochemically aged diesel and wood combustion particles.

2 Experimental setup

The PSI smog chamber is a 27 m^3 ($3 \times 3 \times 3$ m) flexible bag made of 125 µm thickness DuPont Teflon fluorocarbon film (FEP, type 500A, Foiltec GmbH, Germany). The Teflon bag is temperature controlled by two cooling units that keep the temperature between 20 and 25 °C. Diesel and wood burning emission particles are injected into the smog chamber, where they can be characterized. Solar radiation was simulated by four xenon arc light sources. The chamber is equipped with several instruments to monitor the particle and the gas phase during an experiment. More details about the PSI smog chamber are given in Paulsen et al. (2005). The experimental setup used during the PSI IMBALANCE campaign 2009 is shown in Fig. 1 and the complete overview for the diesel and wood burning experiments can be found in Chirico et al. (2010) and Heringa et al. (2011), respectively.

ACPD
12, 14697–14726, 2012

2.1 Methodology

During the measurement period, diesel experiments took place from 17 August to 4 September 2009 where two diesel vehicles were used as emission sources. A EURO3 Opel Astra with a diesel oxidation catalyst (DOC) but no particle filter was used to produce soot particles from 17 August to 26 August. From 31 August to 4 September, a EURO2 Volkswagen Transporter TDI Syncro with no emission after-treatment was used. More details about the source emission conditions are given in Table 1.

Wood burning experiments took place from 9 to 23 September 2009. A modern log wood burner was used during this period in order to reproduce the emissions resulting from house heating. It was possible to sample and investigate three phases: the starting, flaming and smoldering phase. The latter was not investigated during this study as the smoldering phase is primarily gas phase. The starting phase refers to particles that were directly injected after the wood started to burn in the chimney. The flaming phase corresponds to particles which were injected after the wood was completely flaming. Table 2 summarizes the days and conditions of each experiments.

Generated particles were directed through a dilution system in order to reduce the total number concentration of particles produced. The dilution system was heated to 150 °C in order to keep the combustion products close to the temperature of the car or chimney exhaust before injecting them into the smog chamber in order to avoid any condensation of VOCs that resulted from the combustion.

Products resulting from the combustion are mainly black carbon (BC), OC and VOCs. Note that another abundant compound present in diesel vehicle emissions (and not in wood burning emissions) is NO. Primary particles were characterized for 1 to 2 h before triggering photochemical reaction. In the case of the diesel experiments, ozone was first injected in order to accelerate the depletion of NO to form NO_2. The four xenon arc lights were then switched on to simulate solar radiation and oxidized the VOCs. Propene was introduced to have a favorable NO_2 to VOC ratio to form radicals and avoid formation of nitric acid (HNO_3). Soot particles are coated via condensation of the

ACPD
12, 14697–14726, 2012

oxidized VOCs from their own gas phase. Due to the very low content of NO from wood combustion, neither ozone or propene needed to be injected into the smog chamber. Lights were switched on to trigger photochemical reactions after the characterization of primary particles. Note that α-pinene was injected as additional VOC during only one experiment (15d) after 5.5 h lights being on in order to add a thicker coating to the particles.

More details on the particulate organic mass and black carbon measurements are given in Chirico et al. (2010) and Heringa et al. (2011). The OC concentrations were derived from aerosol mass spectrometer data using the procedure as described in Aiken et al. (2008). Size distributions of the particles were measured with a Scanning Mobility Particle Sizer (SMPS, TSI Model 3071) from where the mean mobility diameter of the particles was derived. More information about the particles hygroscopicity measurements can be found in Tritscher et al. (2011) and Martin et al. (2012).

2.2 IN measurements

Ice nuclei measurements were performed with the Portable Ice Nucleation Chamber (PINC) which was connected downstream of the PSI smog chamber (see Fig. 1). Briefly, the instrument consists of two parallel vertical plates with a spacing of 10 mm which can be individually temperature controlled. The inner walls are coated with a thin layer of ice and set at a similar temperature before a measurement is conducted. Aerosols are then sampled at a flow of 1 liter per min ($l\,min^{-1}$) between two dry particle-free sheath air layers (4.5 $l\,min^{-1}$ each). The difference between the warm and cold plate temperature is then progressively increased to create a supersaturation profile between the two walls. A higher temperature difference produces a higher supersaturation that the particles are exposed to. Ice crystals are detected by their larger size (relative to the aerosol particles sampled) with an optical particle counter (OPC, CLIMET 3100). Above water saturation in the growth section of PINC, particles that form water droplets will evaporate before they are sampled by the OPC due to the presence of an evaporation section held at water sub-saturation, upstream of the

ACPD
12, 14697–14726, 2012

OPC. However, above a certain supersaturation with respect to water, the residence time of the particles in the evaporation section is not long enough to evaporate the droplets. This is termed as the droplet survival point where ice crystals cannot be differentiated from water droplets by their size alone. A detailed description of PINC can be found in Chou et al. (2011). PINC is able to measure quantitatively ice nucleation in the deposition mode when the relative humidity with respect to water RH_w at the sample position is below 100 % and condensation freezing when RH_w is above 100 %. Nevertheless, in the latter case, it is difficult to distinguish the fraction of ice crystals formed via condensation freezing if deposition was already occurring at lower RH. If no ice formation was observed before water saturation, we attribute the ice formation at water supersaturated conditions to condensation freezing.

It has been shown by previous studies (DeMott et al., 1999; Möhler et al., 2005b,a; Dymarska et al., 2006) that deposition ice nucleation onto soot particles is not observed at temperatures above −30 °C. Therefore, the ice nucleation ability of combustion particles in this study was investigated at three nominal temperatures, −30 °C, −35 °C and −40 °C. The uncertainties in the calculated RH_w at water saturation for this sampling temperature range is on the order of 3 %.

3 Results and discussion

Investigation of the ice nucleation properties of two different types of diesel vehicles emission particles was conducted (following the EURO3 and EURO2 norms). More information on these norms can be found at http://europa.eu/legislation_summaries/environment/air_pollution/index_en.htm. Figure 2 shows the different RH conditions at which we observed ice active fractions (0.1 %, 0.5 % and 1 %) of freshly emitted diesel particles as a function of temperature and vehicle type. This comparison has also been done for wood burning particles (but only for the photochemically aged due to the few available data of the freshly emitted particles) sampled from the starting and flaming phase. In Fig. 3 the results for 0.1, 1 and 5 % ice active fractions as a function of

ACPD
12, 14697–14726, 2012

temperature are shown. It is crucial to mention for the rest of the discussion that the ice active fractions are normalized to the particles with a diameter larger than 50 nm in order to remove the contribution from nucleation mode particles that form in the photochemical process. We note that there is no significant difference between the ice activity of the starting and the flaming phase. Due to similar ice nucleation properties of the different vehicle types and wood burning phases, we decided for the rest of the discussion to average the values of both types of vehicles emission for the diesel experiments and to also average the values for both phases of the wood burning experiments in order to facilitate the discussion on the photochemical effect at different temperatures.

3.1 Ice nucleation ability of diesel particles

The ice nucleation results of fresh and photochemically aged diesel particles are shown in Fig. 4. At −30 °C and −35 °C, we conclude that no detectable ice nucleation is taking place since the 1 % activated fraction appears above the droplet survival line. At −40 °C, ice formation occurs slightly below water saturation via deposition nucleation at 137 % RH_i and 92 % RH_w. This is comparable to the studies by Möhler et al. (2005b) and Kanji et al. (2011) conducted with graphite spark soot where the necessary relative humidities required to reach a 0.1 % ice active fraction is in the same in the same order, i.e ≈ 87 %–95 % RH_w at −40 °C (see Fig. 6 for comparison). Photochemical aging of particles did not inhibit the ice nucleation properties. Furthermore, at −40 °C, ice nucleation onto aged particles took place at similar relative humidities to non aged particles. This similarity may be explained by the fact that throughout these experiments, the organic coating onto the diesel particles was not thick enough to de-activate or enhance the ice nucleation properties of the aerosol. It is also possible due to the chain like shape of soot that the coating was not uniform and that some spots on the particles were not coated and thus no change in IN ability could be observed.

Figure 7a shows the ice activated fraction of aged diesel particles of experiment 15d at different times of the experiment. Ice nucleation was not observed after

ACPD
12, 14697–14726, 2012

photochemical aging, but was then observed at −35 °C in the condensation freezing mode after addition and photochemical reaction of α-pinene, which infers that parameters like the chemical composition or the size is enhancing the IN ability of the particles. This also suggests a thicker and more uniform coating distribution around the particles. Figure 7b shows the mean mobility diameter derived from the SMPS measurements throughout experiment 15d, and it is noticeable that after α-pinene was added the mean diameter substantially increased confirming that the size of the particle possibly plays a role in the IN ability enhancement. Regarding the composition, the OC:BC ratio also increased from 0.7 to 1.58, after addition of α-pinene. The effect on the IN ability of the size and the OC:BC ratio are discussed more in detail in Sect. 3.3.

3.2 Ice nucleation ability of wood burning particles

Figure 5 shows the ice nucleation ability of freshly emitted and photochemically aged wood particles. At −30 °C, no detectable ice nucleation can be inferred. This result is in agreement with the study from Petters et al. (2009) where biomass burning of several grasses and wood types were investigated at −30 °C and did not show any detectable ice crystal formation. Unlike diesel particles, at −35 °C wood burning particles show significant ice formation in the condensation freezing mode. The effect of coating seems to decrease the ice nucleation ability of the particles but is still similar to the uncoated particles within the uncertainties in RH of PINC (±3 %). At −40 °C, deposition nucleation takes place on both fresh and aged wood burning particles at similar relative humidity conditions ($RH_w \approx 92\,\%$–$96\,\%$). These conditions are also similar to those at which fresh and aged diesel particles trigger ice nucleation and thus also similar to graphite spark generated soot (Möhler et al., 2005b; Kanji et al., 2011). This brings new questions as: is there a unique relative humidity threshold for when polydisperse soot and biomass burning particles may act as ice nuclei in the deposition nucleation mode? This is discussed in more details in Sect. 3.4.

ACPD
12, 14697–14726, 2012

3.3 Comparison between wood and diesel particles

Our study has shown that photochemical aging with its own VOC gas phase has no observable effect on the ice nucleation ability of both diesel and wood burning particles, except in experiment 15d where a thick organic coating of oxidized α-pinene was present. It is unclear as to why wood burning particles are more ice active at $-35\,^{\circ}C$ compared to diesel particles. In an attempt to explain this behavior, the OC:BC ratio in our work was investigated as Möhler et al. (2005b) showed that the particle OC:BC ratio is an important parameter to consider for IN properties of soot particles. The evolution of the OC:BC ratio of diesel experiments is shown in Fig. 8. The ratio is approximately 0.15 for the Opel Astra, where as the VW transporter showed higher values between 0.2 to 0.4 after turning on the smog chamber's xenon lights. The only exception concerns experiment 15d, where a large amount of OC was produced after photochemistry and values up to 0.7 were reached. Note that in experiment 15d, no exhaust after-treatment devices were used. More details about the organic matter (OM) variations are discussed in Chirico et al. (2010), and are not the focus of this paper. Nevertheless, no ice nucleation was observed at this high OC:BC ratio, and could only be observed when the sizes of the particles as well as the OC:BC ratio increased (increments from a mean diameter of 130 nm to 180 nm and from an OC:BC of 0.7 to above 1.5). In comparison, the OC:BC ratio of wood burning particles shows different behaviors depending of the phase sampled as it is depicted in Fig. 9. For the flaming phase experiments, the OC:BC ratio varies between 0.1 to 0.5 which is in the same range as the diesel experiments. Nevertheless, ice nucleation was observed for those experiments at $-35\,^{\circ}C$ whereas no ice was formed for the diesel experiments. Indications that the OC:BC ratio is not playing an important role in the ice nucleation efficiency are also confirmed by the starting phase experiments, which show an ice nucleation behavior similar to the flaming phase experiments, but show a OC:BC ratio above 2. From these observations, we conclude that the better IN ability observed in experiment 15d is mainly attributed to the increase in the size of the particles.

ACPD
12, 14697–14726, 2012

One explanation of the differences in the ice nucleation behavior at −35 °C could be attributed to a generally larger average size of the wood burning particles compared to diesel particles and a broader size distribution which explains that for a similar OC:BC ratio, wood burning particles formed ice crystals at −35 °C. Another explanation could also be the different chemical composition of the products resulting from the combustion. It is known for example that emissions from wood pellets burning usually show a higher fraction of fly ash which probably have a better ice nucleation activity than soot particles.

3.4 Homogeneous or heterogeneous ice formation?

An interesting feature of Fig. 7 that was also found in all the experiments at −40 °C for diesel and wood burning particles, as well as wood burning experiments at −35 °C, is the steepness of the activation curve. Recently Friedman et al. (2011) assumed in their experiment that the ice crystals observed at −40 °C are formed via homogeneous nucleation. Our experiments showed some similar behavior with an ice activation of 0.1 % starting at around a RH_i of 137 % and RH_w of 92 % at −40 °C for both wood and diesel particles. The true nature of the mechanism that is occurring is however uncertain as ice was observed at RH conditions below the predicted homogeneous nucleation line (as is evident in Fig. 3) for a 200 nm ammonium sulphate (AS) particle (Koop et al., 2000). Furthermore, due to the non-hygroscopic nature of the particles investigated (Tritscher et al., 2011; Martin et al., 2012) and the absence of soluble material, the hypothesis of homogeneous nucleation taking place below the predicted homogeneous nucleation threshold for AS is difficult to prove. Therefore, we conclude that deposition nucleation is taking place, but further investigations to assess the nature of the mechanism would be required in future experiments.

ACPD
12, 14697–14726, 2012

3.5 Comparison with mineral dust

Figure 10 shows a comparison of the IN activity of the particles investigated during IMBALANCE to the one of different mineral dust types. It is observed that fresh diesel and wood burning particles require higher supersaturation with respect to ice and water to reach a 0.1 % activated fraction for the temperature range from −30 °C to −40 °C. At −40 °C Arizona test dust (ATD) and Canary Island dust (CID) reach the 0.1 % ice active fraction at much lower RH_w (by 10 to 25 %). Furthermore, deposition freezing takes place at temperatures as warm as −30 °C and close to water saturation on ATD, CID and Saharan dust (SD). This feature is not observable on either diesel or wood burning particles at −30 °C and −35 °C as they either form ice via condensation freezing or did not form detectable ice crystals as discussed in previous sections. Note that no information on the ice formation mechanism and conditions required are available for Israeli dust (ID) as no experiments below −30 °C had been conducted. It is therefore possible to conclude that diesel and wood burning particles are poorer IN than mineral dust in the temperature range studied.

4 Conclusions

Investigation of the ice nucleation properties of diesel and wood burning particles have been conducted from 17 August 2009 until 23 September 2009 at the Paul Scherrer Institute smog chamber. The first set of results showed that the ice nucleation ability of the particles did not differ as a function of the burning phase or diesel vehicle type investigated. Furthermore, the results showed that for diesel particles, ice formation took place only at temperatures as low as −40 °C by deposition nucleation. Wood burning particles did nucleate ice above water saturation at −35 °C via condensation freezing and via deposition nucleation at −40 °C, below water saturation. Investigations of the effect of photochemistry on both particle types have also been conducted. Results show that photochemical aging did not result in any significant changes in the ice nucleation

ACPD
12, 14697–14726, 2012

ability of the particles, unlike the studies from DeMott et al. (1999) and Möhler et al. (2005a) where they found that sulfuric acid coating either enhanced or decreased the ice nucleation onset of soot particles. Photochemical aging from the gas phase of its own exhaust could lead to the lack of uniform coating and could be the explanation as why no difference was observed between fresh and aged particles. This assumption is confirmed by experiment 15d where a thicker coating after addition of α-pinene led to a larger particle size, a higher OC:BC ratio and a better IN ability. After investigation we believe that the size of the particles could be the key parameter to the increase in ice nucleation efficiency rather than the OC:BC ratio, as the particles from the flaming phase experiments showed ice nucleation at −35 °C despite their low OC:BC ratio (0.1 to 0.5).

Wood burning and diesel combustion particles are emitted in the atmosphere in very high concentrations which make them a potential source of IN at mixed phase cloud levels. Our study has shown that ice formation could not be observed at −30 °C but is observable in some cases at −35 °C for fresh and photochemically aged particles. Photo-oxidation of the particles was performed at atmospherically relevant conditions in the PSI smog chamber and no modification of IN ability on the particles was observed. It is therefore possible to conclude that diesel and wood burning particles do not play a significant role in heterogeneous ice formation at mixed phase clouds temperatures in comparison to mineral dust. It would nevertheless be worthwhile to investigate the effect of photochemistry onto diesel and wood burning particles at temperatures below −40 °C in order to see if this has an impact for colder clouds.

Acknowledgements. We acknowledge the support by the IMBALANCE project of the Competence Center Environment and Sustainability of the ETH Domain (CCES). We also acknowledge Hannes Wydler for the various technical help provided on the instrument.

ACPD
12, 14697–14726, 2012

References

Aiken, A., DeCarlo, P., Kroll, J., Worsnop, D., Huffman, J., Docherty, K., Ulbrich, I., Mohr, C., Kimmel, J., Sueper, D., Sun, Y., Zhang, Q., Trimborn, A., Northway, M., Ziemann, P., Canagaratna, M., Onasch, T., Alfarra, M., Prévôt, A., Dommen, J., Duplissy, J., Metzger, A., Baltensperger, U., and Jimenez, J.: O/C and OM/OC ratios of primary, secondary, and ambient organic aerosols with high-resolution time-of-flight aerosol mass spectrometry, Environ. Sci. Technol., 42, 4478–4485, 2008. 14703

Chirico, R., DeCarlo, P. F., Heringa, M. F., Tritscher, T., Richter, R., Prévôt, A. S. H., Dommen, J., Weingartner, E., Wehrle, G., Gysel, M., Laborde, M., and Baltensperger, U.: Impact of aftertreatment devices on primary emissions and secondary organic aerosol formation potential from in-use diesel vehicles: results from smog chamber experiments, Atmos. Chem. Phys., 10, 11545–11563, doi:10.5194/acp-10-11545-2010, 2010. 14701, 14703, 14707, 14715

Chou, C., Stetzer, O., Weingartner, E., Jurányi, Z., Kanji, Z. A., and Lohmann, U.: Ice nuclei properties within a Saharan dust event at the Jungfraujoch in the Swiss Alps, Atmos. Chem. Phys., 11, 4725–4738, doi:10.5194/acp-11-4725-2011, 2011. 14704

Cozic, J., Mertes, S., Verheggen, B., Cziczo, D., Gallavardin, S., Walter, S., Baltensperger, U., and Weingartner, E.: Black carbon enrichment in atmospheric ice particle residuals observed in lower tropospheric mixed phase clouds, J. Geophys. Res, 113, D15209, doi:10.1029/2007JD009266, 2008. 14699

DeMott, P., Chen, Y., Kreidenweis, S., Rogers, D., and Sherman, D.: Ice formation by black carbon particles, Geophys. Res. Lett., 26, 2429–2432, doi:10.1029/1999GL900580, 1999. 14700, 14704, 14710

Demott, P., Möhler, O., Stetzer, O., Vali, G., Levin, Z., Petters, M., Murakami, M., Leisner, T., Bundke, U., Klein, H., Kanji, Z. A., Cotton, R., Jones, H., Benz, S., Brinkmann, M., Rzesanke, D., Saathoff, H., Nicolet, M., Saito, A., Nillius, B., Bingemer, H., Abbatt, J., Ardon, K., Ganor, E., Georgakopoulos, D. G., and Saunders, C.: Resurgence in ice nuclei measurement research, B. Am. Meteorol. Soc., 92, 1623–1635, 2011. 14726

Denman, K. L., Brasseur, G., Chidthaisong, A., Ciais, P., Cox, P. M., Dickinson, R. E., Hauglustaine, D., Heinze, C., Holland, E., Jacob, D., Lohmann, U., Ramachandran, S., da Silva Dias, P. L., Wofsy, S. C., and Zhang, X.: Couplings Between Changes in the Climate System and Biogeochemistry. In: Climate Change 2007: The Physical Science Basis. Contribution of

ACPD
12, 14697–14726, 2012

Working Group I to the Fourth Assessment Report of the Intergovernmental Panel on Climate Change, edited by: Solomon, S., Qin, D., Manning, M., Chen, Z., Marquis, M., Averyt, K. B., Tignor, M., and Miller, H. L., Cambridge University Press, Cambridge, United Kingdom and New York, NY, USA, 2007. 14699

Dymarska, M., Murray, B., Sun, L., Eastwood, M., Knopf, D., and Bertram, A.: Deposition ice nucleation on soot at temperatures relevant for the lower troposphere, J. Geophys. Res.-Atmos., 111, D04204, doi:10.1029/2005JD006627, 2006. 14700, 14704

Ebert, M., Worringen, A., Benker, N., Mertes, S., Weingartner, E., and Weinbruch, S.: Chemical composition and mixing-state of ice residuals sampled within mixed phase clouds, Atmos. Chem. Phys., 11, 2805–2816, doi:10.5194/acp-11-2805-2011, 2011. 14699

Friedman, B., Kulkarni, G., Beránek, J., Zelenyuk, A., Thornton, J., and Cziczo, D.: Ice nucleation and droplet formation by bare and coated soot particles, J. Geophys. Res., 116, D17203, doi:10.1029/2011JD015999, 2011. 14708

Hansen, J., Sato, M., and Ruedy, R.: Radiative forcing and climate response, J. Geophys. Res., 102, 6831–6864, 1997. 14699

Heringa, M. F., DeCarlo, P. F., Chirico, R., Tritscher, T., Dommen, J., Weingartner, E., Richter, R., Wehrle, G., Prévôt, A. S. H., and Baltensperger, U.: Investigations of primary and secondary particulate matter of different wood combustion appliances with a high-resolution time-of-flight aerosol mass spectrometer, Atmos. Chem. Phys., 11, 5945–5957, doi:10.5194/acp-11-5945-2011, 2011. 14701, 14703, 14716

Hoose, C., Lohmann, U., Erdin, R., and Tegen, I.: The global influence of dust mineralogical composition on heterogeneous ice nucleation in mixed-phase clouds, Environ. Res. Lett., 3, 025003, doi:10.088/1748-9326/3/2/025003, 2008. 14700

Kamphus, M., Ettner-Mahl, M., Klimach, T., Drewnick, F., Keller, L., Cziczo, D. J., Mertes, S., Borrmann, S., and Curtius, J.: Chemical composition of ambient aerosol, ice residues and cloud droplet residues in mixed-phase clouds: single particle analysis during the Cloud and Aerosol Characterization Experiment (CLACE 6), Atmos. Chem. Phys., 10, 8077–8095, doi:10.5194/acp-10-8077-2010, 2010. 14699

Kanji, Z. A., DeMott, P. J., Möhler, O., and Abbatt, J. P. D.: Results from the University of Toronto continuous flow diffusion chamber at ICIS 2007: instrument intercomparison and ice onsets for different aerosol types, Atmos. Chem. Phys., 11, 31–41, doi:10.5194/acp-11-31-2011, 2011. 14705, 14706, 14722, 14726

ACPD
12, 14697–14726, 2012

Kärcher, B., Möhler, O., DeMott, P. J., Pechtl, S., and Yu, F.: Insights into the role of soot aerosols in cirrus cloud formation, Atmos. Chem. Phys., 7, 4203–4227, doi:10.5194/acp-7-4203-2007, 2007. 14700

Koop, T., Luo, B., Tsias, A., and Peter, T.: Water activity as the determinant for homogeneous ice nucleation in aqueous solutions, Nature, 406, 611–614, 2000. 14708, 14720

Koren, I., Kaufman, Y., Remer, L., and Martins, J.: Measurement of the effect of Amazon smoke on inhibition of cloud formation, Science, 303, 1342, doi:10.1126/science.1089424, 2004. 14699

Lin, J., Matsui, T., Pielke Sr, R., and Kummerow, C.: Effects of biomass-burning-derived aerosols on precipitation and clouds in the Amazon Basin: a satellite-based empirical study, J. Geophys. Res., 111, D19204, doi:10.1029/2005JD006884, 2006. 14699

Lohmann, U. and Hoose, C.: Sensitivity studies of different aerosol indirect effects in mixed-phase clouds, Atmos. Chem. Phys., 9, 8917–8934, doi:10.5194/acp-9-8917-2009, 2009. 14699

Martin, M., Tritscher, T., Jurányi, J., Heringa, M. F., Sierau, B., Weingartner, E., Chirico, R., Gysel, M., Prévôt, A. S. H., Baltensperger, U., and Lohmann, U.: Hygroscopic properties of fresh and aged wood burning particles, J. Aerosol Sci., JAS, submitted, 2012. 14703, 14708

McDonald, J., Zielinska, B., Fujita, E., Sagebiel, J., Chow, J., and Watson, J.: Fine particle and gaseous emission rates from residential wood combustion, Environ. Sci. Technol., 34, 2080–2091, 2000. 14699

Möhler, O., Büttner, S., Linke, C., Schnaiter, M., Saathoff, H., Stetzer, O., Wagner, R., Krämer, M., Mangold, A., Ebert, V., and Schurath, U.: Effect of sulfuric acid coating on heterogeneous ice nucleation by soot aerosol particles, J. Geophys. Res., 110, D11210, doi:10.1029/2004JD005169, 2005a. 14700, 14704, 14710

Möhler, O., Linke, C., Saathoff, H., Schnaiter, M., Wagner, R., Mangold, A., Krämer, M., and Schurath, U.: Ice nucleation on flame soot aerosol of different organic carbon content, Meteorol. Z., 14, 477–484, 2005b. 14700, 14704, 14705, 14706, 14707, 14722

Paulsen, D., Dommen, J., Kalberer, M., Prévôt, A. S. H., Richter, R., Sax, M., Steinbacher, M., Weingartner, E., and Baltensperger, U.: Secondary organic aerosol formation by irradiation of 1,3,5-Trimethylbenzene-NO_x-H_2O in a new reaction chamber for atmospheric chemistry and physics, Environ. Sci. Technol., 39, 2668–2678, 2005. 14701

Petters, M., Parsons, M., Prenni, A., DeMott, P., Kreidenweis, S., Carrico, C., Sullivan, A., McMeeking, G., Levin, E., Wold, C., Collett Jr., J. L., and Moosmüller, H.: Ice nuclei emis-

ACPD
12, 14697–14726, 2012

sions from biomass burning, J. Geophys. Res., 114, D07209, doi:10.1029/2008JD011532, 2009. 14706
Schauer, J., Kleeman, M., Cass, G., and Simoneit, B.: Measurement of emissions from air pollution sources. 3. C1–C29 organic compounds from fireplace combustion of wood, Environ. Sci. Technol., 35, 1716–1728, 2001. 14699
Schauer, J., Kleeman, M., Cass, G., and Simoneit, B.: Measurement of emissions from air pollution sources. 5. C1–C32 organic compounds from gasoline-powered motor vehicles, Environ. Sci. Technol., 36, 1169–1180, 2002. 14699
Storelvmo, T., Kristjánsson, J., and Lohmann, U.: Aerosol influence on mixed-phase clouds in CAM-Oslo, J. Atmos. Sci., 65, 3214–3230, 2008. 14700
Targino, A., Coe, H., Cozic, J., Crosier, J., Crawford, I., Bower, K., Flynn, M., Gallagher, M., Allan, J., Verheggen, B., Baltensperger, U., and Chourlaton, T.: Influence of particle chemical composition on the phase of cold clouds at a high-alpine site in Switzerland, J. Geophys. Res., 114, D18206, doi:10.1029/2008JD011365, 2009. 14699
Tritscher, T., Jurányi, Z., Martin, M., Chirico, R., Gysel, M., Heringa, M., DeCarlo, P., Sierau, B., Prévôt, A., Weingartner, E., and Baltensperger, U.: Changes of hygroscopicity and morphology during ageing of diesel soot, Environ. Res. Lett., 6, 034026, doi:10.1088/1748-9326/6/3/034026, 2011. 14703, 14708
Vali, G.: Nucleation terminology, B. Am. Meteorol. Soc., 66, 1426–1427, 1985. 14699

ACPD
12, 14697–14726, 2012

Table 1. Summary of the diesel experiments. The experiment number refers to the ones used in Chirico et al. (2010).

Experiment number	date (dd mon yyyy)	comments	mean mobility diameter range
EURO3, Opel Astra, with DOC, idle conditions			
8d	17 Aug 2009	warm idle	100 to 160 nm
9d	19 Aug 2009		80 to 160 nm
10d	21 Aug 2009		
11d	26 Aug 2009		80 to 160 nm
EURO2, VW Transporter, without after-treatment, idle conditions			
13d	31 Aug 2009		60 to 130 nm
14d	02 Sep 2009		60 to 150 nm
15d	04 Sep 2009	α-pinene added	60 to 180 nm

ACPD
12, 14697–14726, 2012

Table 2. Summary of the wood burning experiments. The experiment number refers to the ones used in Heringa et al. (2011).

Experiment number	date (dd mon yyyy)	comments	mean mobility diameter range
Modern log wood burner			
11w	09 Sep 2009	flaming phase	110 to 140 nm
12w	11 Sep 2009	flaming phase	150 to 200 nm
13w	16 Sep 2009	flaming phase	180 to 270 nm
15w	21 Sep 2009	starting phase	140 to 220 nm
16w	23 Sep 2009	starting phase	100 to 160 nm

ACPD
12, 14697–14726, 2012

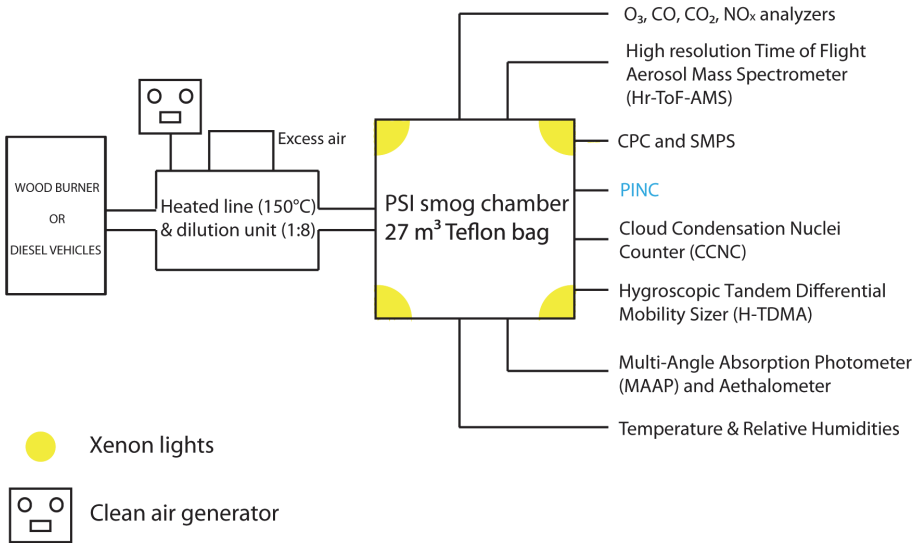

Fig. 1. Experimental setup during the IMBALANCE campaign, 2009.

ACPD
12, 14697–14726, 2012

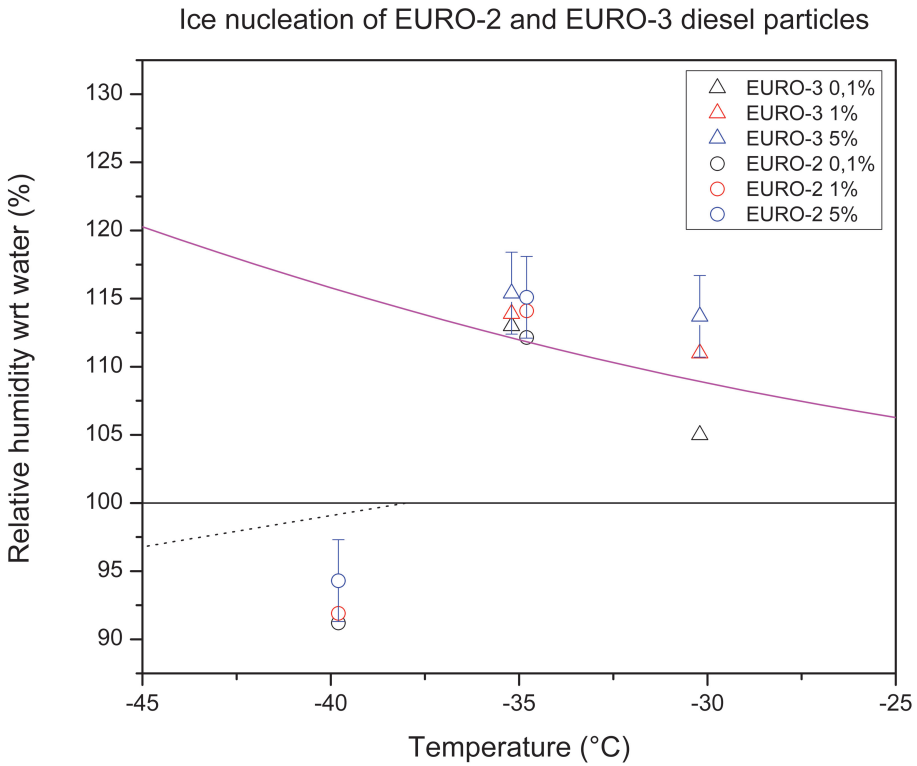

Fig. 2. Relative humidity with respect to (wrt) water as a function of temperatures at which different ice fraction are detected: 0.1 %, 1 % and 5 % activated fraction for EURO-2 and EURO-3 diesel vehicles. The magenta line represents the droplet survival line above which ice and water are both detected by optical means. The dotted line represents the homogeneous freezing threshold for supercooled solution droplets.

ACPD
12, 14697–14726, 2012

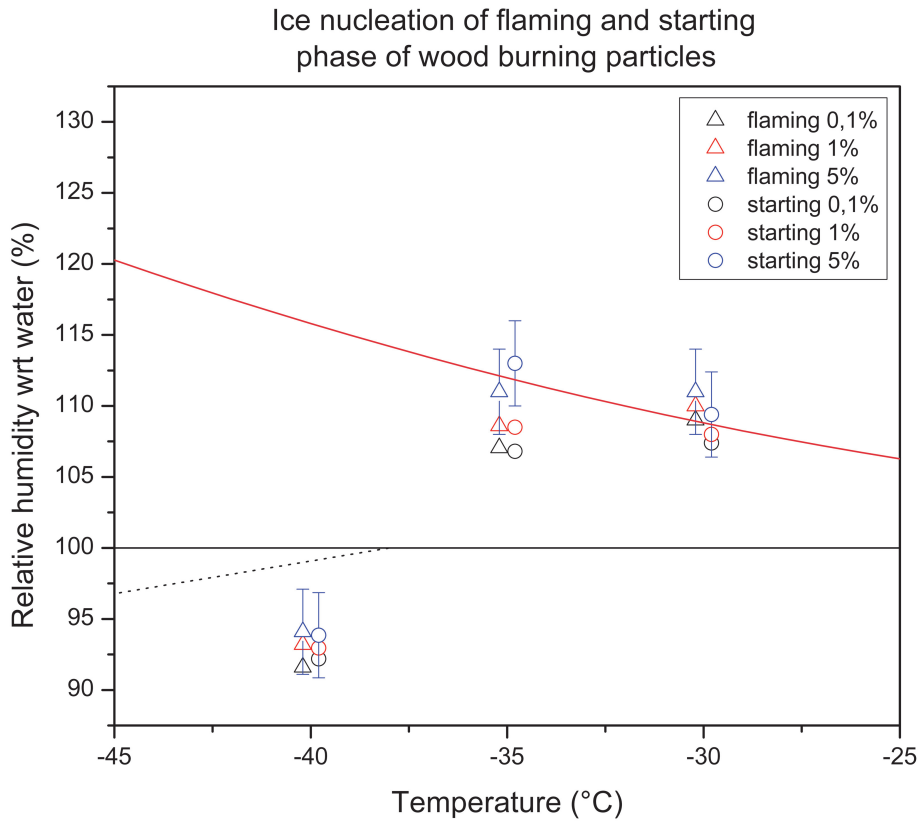

Fig. 3. As Fig. 2 but for wood burning particles in both the flaming and starting phase.

ACPD
12, 14697–14726, 2012

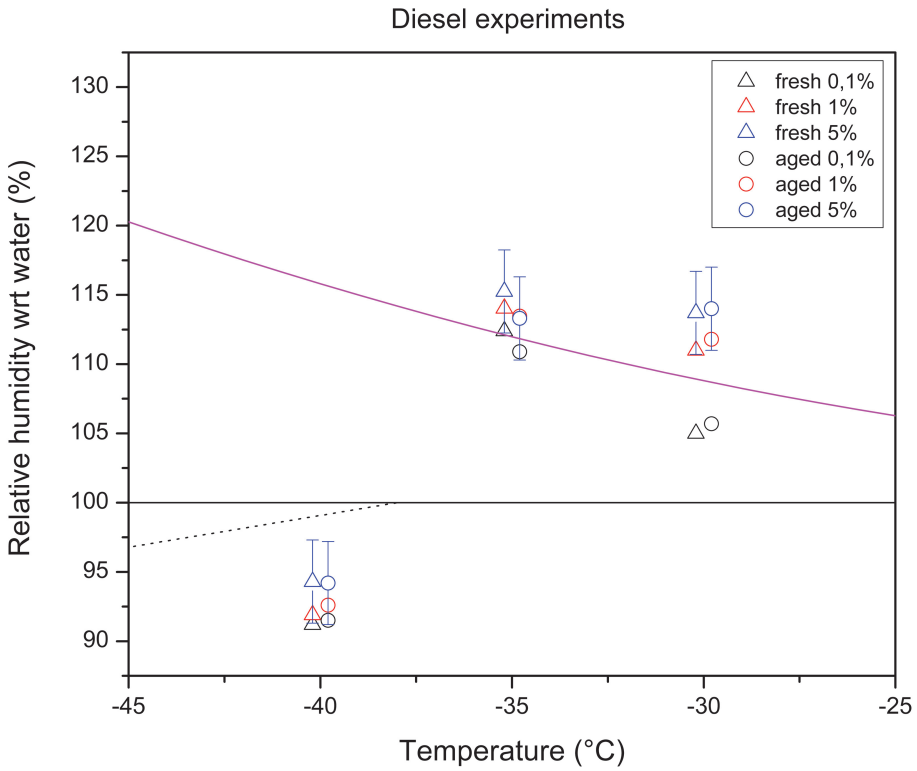

Fig. 4. Ice onset relative humidity for deposition/condensation freezing as a function of temperature for the given ice active fractions. Data shown are for fresh and photochemically aged diesel particles. The magenta line represents the droplet survival line above which ice and water are both detected by the optical particle counter. The dotted line represents the homogeneous freezing threshold for 200 nm supercooled ammonium sulphate solution based on the parameterizations of Koop et al. (2000).

ACPD
12, 14697–14726, 2012

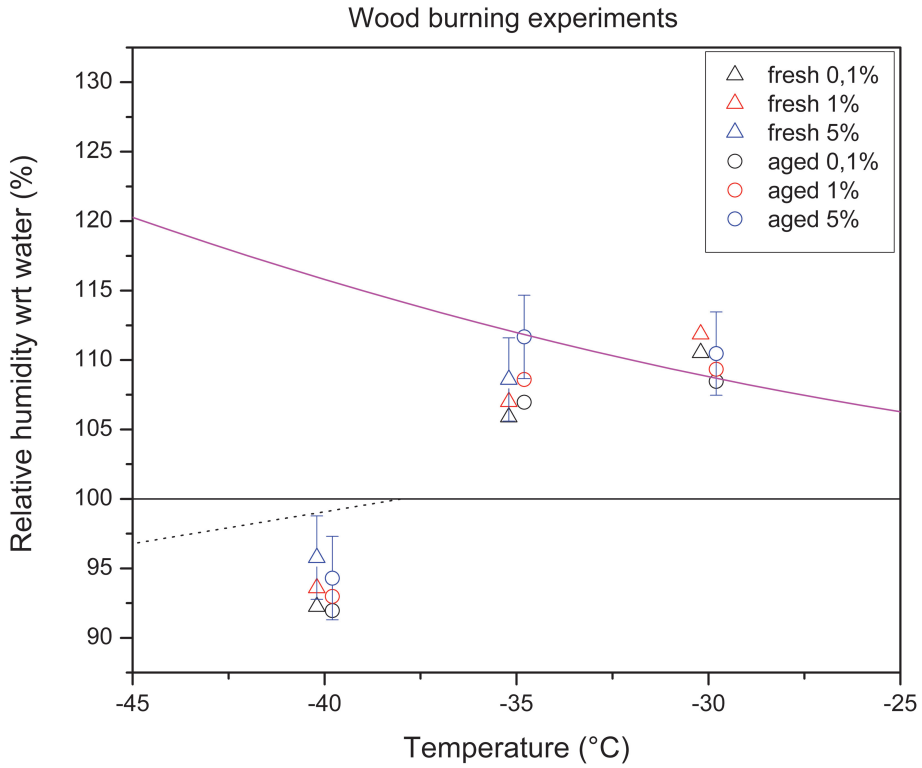

Fig. 5. Same as Fig. 4 but for fresh and photochemically aged wood burning particles.

ACPD
12, 14697–14726, 2012

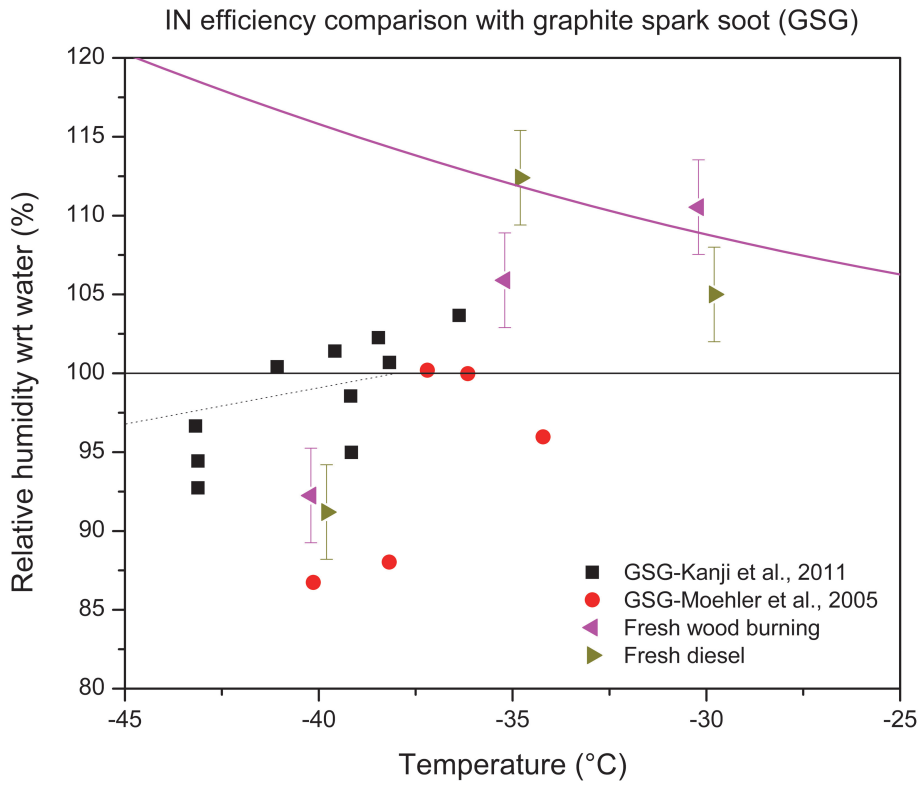

Fig. 6. Ice active fraction of graphite spark soot and fresh diesel and wood burning particles. The data points from Möhler et al. (2005b) are from the AIDA chamber experiments in Karlsruhe, Germany. Those from Kanji et al. (2011) are from the University of Toronto continuous flow diffusion chamber. The magenta and dotted lines represent the same parameters as in Fig. 4. Note that the magenta line is only valid for the wood burning and diesel particles data points.

ACPD
12, 14697–14726, 2012

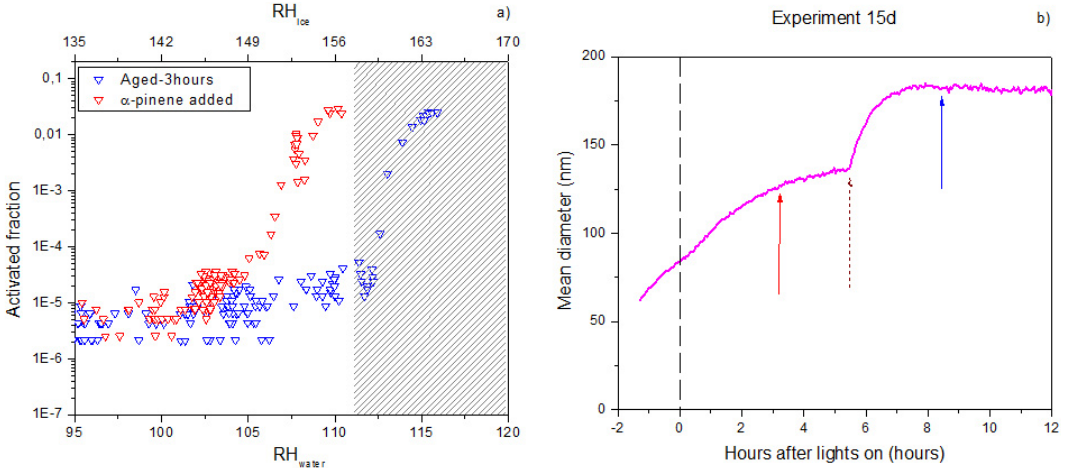

Fig. 7. (a) Ice nucleation activated fraction as a function of saturation ratio with respect to ice and water of photochemically aged diesel particles and diesel particles coated with α-pinene. The shaded area represents the region where the OPC cannot distinguish between ice crystals and water droplets. **(b)** Mean diameter evolution throughout experiment 15d. Solid arrows represent the time where the IN measurements took place and the dotted arrow represent the time when α-pinene was added. The dashed vertical black line represents the moment when lights were turned on.

ACPD
12, 14697–14726, 2012

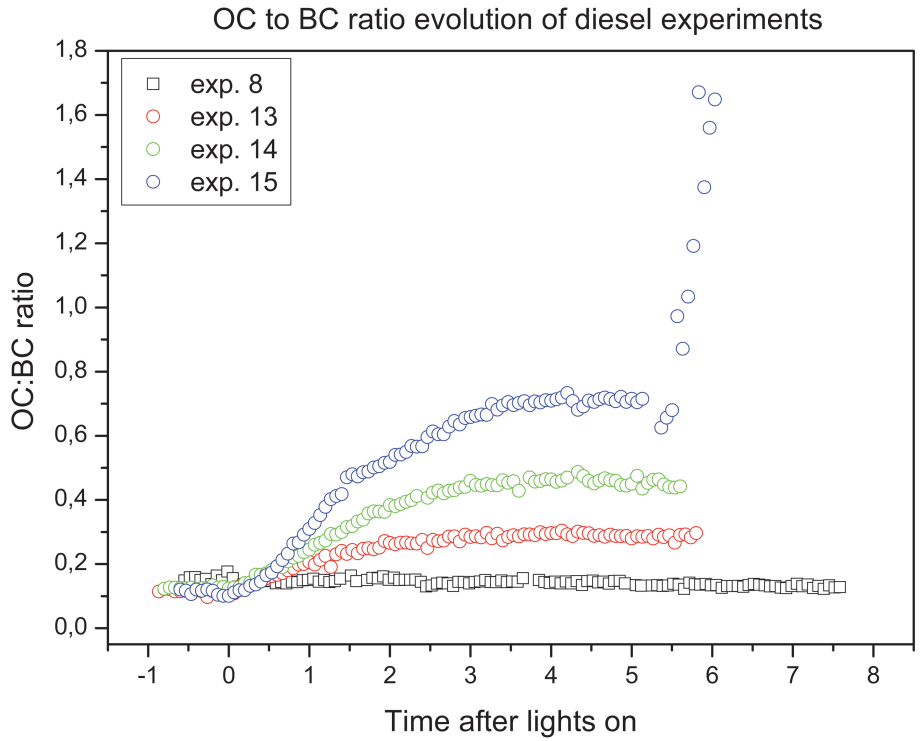

Fig. 8. OC to BC ratio evolution throughout several hours for four diesel experiments. The square symbol represents experiments with the Opel Astra. Circles represent experiments with the VW Transporter.

ACPD
12, 14697–14726, 2012

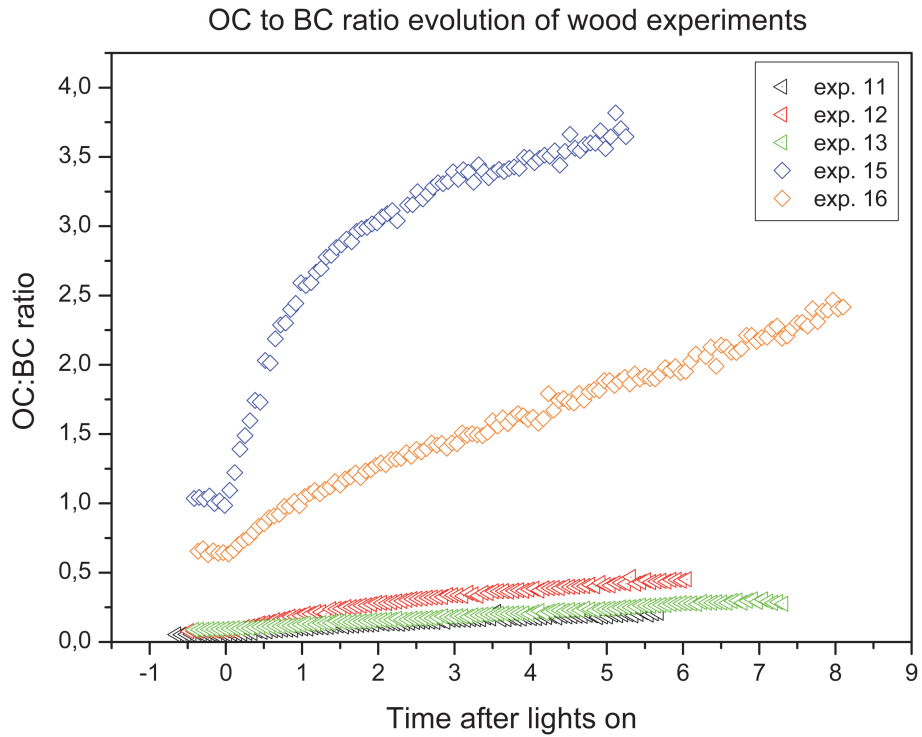

Fig. 9. OC to BC ratio evolution throughout several hours for five wood burning experiments. Triangles correspond to flaming phase experiments. Diamonds correspond to starting phase experiments.

ACPD
12, 14697–14726, 2012

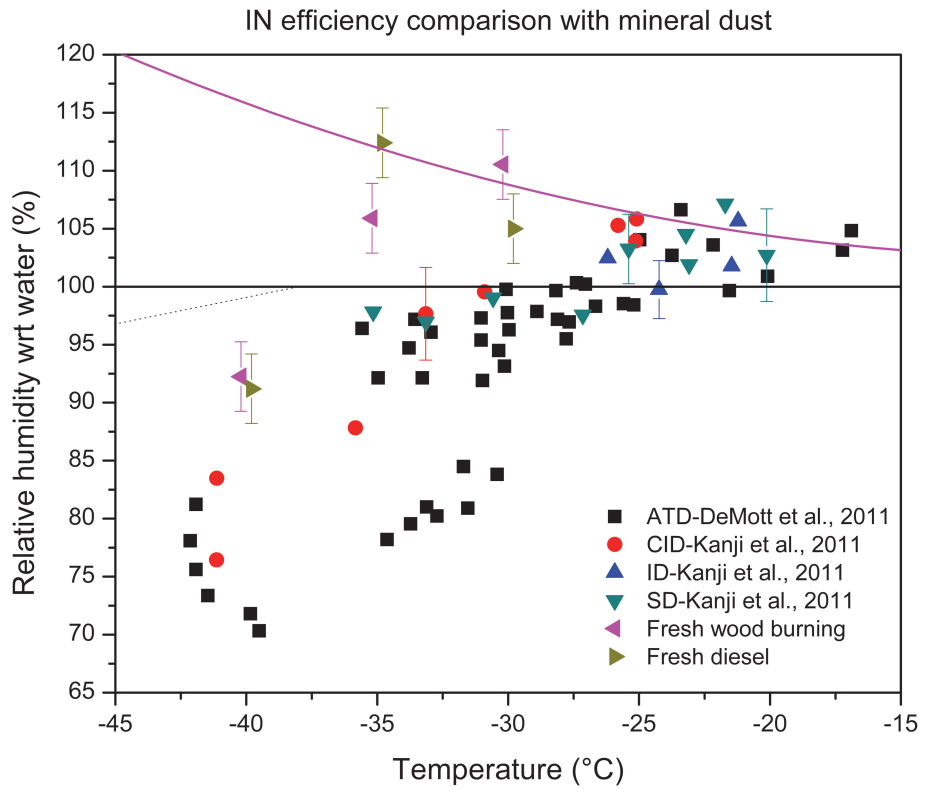

Fig. 10. Ice active fraction of different mineral dust and fresh diesel and wood burning particles. The data points from Demott et al. (2011) are from different IN chamber. Those from Kanji et al. (2011) are from the University of Toronto continuous flow diffusion chamber. The magenta and dotted lines represent the same parameters as in Fig. 4. Note that the magenta line is only valid for the wood burning and diesel particles data points.

ACPD
12, 14697–14726, 2012

Ice nucleation of diesel and wood burning particles

C. Chou et al.